J. Synchrotron Rad. (1995). **2**, 93–98

2*p* X-ray Absorption Spectroscopy in the Earth Sciences

P. F. Schofield,[a] C. M. B. Henderson,[b] G. Cressey[a] and G. van der Laan[c]

[a]Department of Mineralogy, Natural History Museum, Cromwell Road, London SW7 5BD, UK, [b]Department of Geology, University of Manchester, Oxford Road, Manchester M13 9PL, UK, and [c]DRAL, Daresbury Laboratory, Warrington WA4 4AD, UK

(*Received 13 December 1994; accepted 13 January 1995*)

A complete knowledge of 3*d* transition-metal valencies, site occupancies and site symmetries is essential for a full understanding of mineral/melt energetics and behaviour. Over the last few years, significant advances in both instrumentation and theory associated with synchrotron radiation sources and experiments have enabled the development of 2*p* X-ray absorption spectroscopy as a sensitive, element-specific site and valency probe. The potential of this technique in the Earth sciences is discussed in this paper with examples reflecting the variety of problems set by 3*d* transition metals in natural systems.

Keywords: 2*p* XAS; geological materials; valency quantification; site occupancies.

1. Introduction

An understanding of geological and geophysical processes, such as pressure, temperature and redox conditions of crystallization, and element-substitution mechanisms, requires full characterization of the crystalline and non-crystalline materials involved. The thermodynamic and physical properties of these phases all depend upon the interactions at the atomic and sub-atomic levels, hence, a knowledge of the atomic and electronic characteristics of geological materials is essential. While a wide range of modern analytical, diffraction and spectroscopic techniques are available to mineralogists and geochemists, controversial and conflicting ideas regarding site occupancies and valencies in both minerals and geological melts still remain. Most of these techniques possess serious deficiencies based upon variable crystallinity, impurity interference or theoretical limitations, and, consequently, there is still a clear need for a sensitive, element-specific site and valence probe.

Improvement in the instrumentation associated with low-energy synchrotron radiation experiments (<800 eV), particularly in the fields of undulator devices (Padmore & Warwick, 1994) and spherical grating monochromators (Chen & Sette, 1989), has enhanced the application of soft X-ray spectroscopies. In particular, 2*p* ($L_{2,3}$) X-ray absorption spectroscopy (XAS) of 3*d* transition metals probes the electronic structure of these metals, producing a sensitive element-specific probe for both valency and site symmetries (van der Laan & Kirkman, 1992). Indeed this potential has begun to be realized in mineralogical studies relating to valence-state identification (van der Laan, Pattrick, Henderson & Vaughan, 1992; Cressey, Henderson & van der Laan, 1993; Pattrick, van der Laan, Vaughan & Henderson, 1993), valence-ratio quantification (Cressey *et al.*, 1993; Schofield *et al.*, 1994), site symmetries (de Groot *et al.*, 1992) and site occupancies (Schofield, Henderson, Redfern & van der Laan, 1993).

The principles of 2*p* XAS have been described in detail by van der Laan & Kirkman (1992). Their study provides a systematic display and interpretation of calculated 2*p* spectra of the 3*d* transition metals from Ti to Ni, in a variety of valence states, and in both octahedral and tetrahedral crystal fields. 2*p* XAS is based on dipole-allowed, bound-state electron transitions from the core 2*p* level to empty 3*d* states, in effect from the ground state $2p^6\,3d^n$ to the excited state $2p^5\,3d^{n+1}$ configuration. As the Coulomb interaction between the 2*p* and 3*d* electrons is large, the presence, probability and energy of these transitions inherently reflects the local electronic structure, and thus, the $L_{2,3}$ absorption structure contains significant information relating to the valency, symmetry, spin states and crystal-field splitting of the 3*d* transition-metal ions. Other complex transitions can also be observed above the main L_3 structure which produce polaronic satellites, also dependent upon site symmetry, and can provide information on processes such as charge transfer (van der Laan, 1990).

In this paper we will describe how 2*p* XAS is developing into a powerful element-specific valence and site-symmety probe of potential value to mineralogists and geochemists. While the full range of 3*d* transition metals could be described with each element presenting unique problems of different mineralogical and geochemical significance, we have selected a few representative examples to describe the problems, and their solutions, requiring valence-state identification, site-occupancy determination, and valence-state ratio quantification.

2. Identification of valence states

2.1. *Vanadium oxidation states*

The differences between the calculated 2*p* spectra for the ground states possible in different vanadium ions are obvious, as shown in van der Laan & Kirkman (1992).

Chemically complex minerals, however, provide further challenges in that many minerals contain a specific transition metal in multivalent states. In particular, the vanadate group of minerals remain poorly understood due, in part, to the nature (such as rarity, prohibitively small grain sizes, poor diffracting properties) and relative stabilities of the existing material, but also due to the wide range of valencies adopted by the vanadium ions.

Fig. 1 shows the V $L_{2,3}$ absorption spectra of a series of minerals in which, based upon energy shifts alone, four separate oxidation states can be observed. Indeed, these four valence states appear to be present in the mineral corvusite (BM 1957,33) for which a formula of $V_2O_4.6V_2O_5.nH_2O$ was proposed by Henderson & Hess (1933). This formula only requires the presence of V^{5+} and V^{4+}; however, it can be seen that di- and trivalent vanadium are also present calling into question the proposed stoichiometry. While simple crystal chemistry would predict V^{3+} in the mineral montroseite, the 2p spectra also clearly indicate the presence of V^{5+} and V^{2+}. Forbes & Dubessy (1988) stated that Fe is introduced into montroseite as Fe^{2+}, rather than Fe^{3+}, and that the likely oxidation processes require formation of V^{4+}, and that V^{5+}, although possible, was unlikely. Our preliminary results indicate, however, that V^{5+} is present while V^{4+} is absent, and that V^{2+} may also be generated by the charge-balancing process.

The mineral häggite (BM 1963,663) has the unconfirmed formula $V_2O_3.V_2O_4.3H_2O$ (Evans & Mrose, 1960), implying the existence of V^{4+} and V^{3+} which is confirmed by the 2p spectrum in Fig. 1, although it also appears that some V^{2+} may also be present. The relative peak heights of the two components allow a preliminary assessment of the relative proportions of these two oxidation states. When modified by a factor taking account of the ratio of *d* holes in each electronic configuration (the transition intensity being proportional to the number of *d* holes), it appears that these two oxidation states are, indeed, present in approximately equal proportions, as predicted by the proposed formula.

For the minerals hewettite and pucherite only V^{5+} is expected, and for pucherite (BM 45983) this is shown to be the case in Fig. 1; however, the spectrum of hewettite (BM 1972,461) also shows the presence of V^{3+}. The refined structure for hewettite appears to be unreliable (Evans, 1989) which might result from the presence of V oxidation states other than V^{5+}, which in turn might be related to variations in the occupancies of the Ca^{2+} cation site and/or the O(12) anion site. A similar result to this was found by Cressey *et al.* (1993) for the related mineral barnesite, $Na_2V_6O_{16}.3H_2O$, such that only V^{5+} is expected whereas both V^{5+} and V^{3+} are represented in the experimental spectrum.

2.2. *Manganese oxidation states*

The calculated spectra of van der Laan & Kirkman (1992) show significant variations between the different oxidation states for the Mn ions. Mn $L_{2,3}$ absorption edges for a range of minerals (Fig. 2) show how the energy shift can be used to identify individual valency states where several are present in a single sample. The spectrum of schorlomite (BM 32025), in which the Mn is present at the 0.50 wt% MnO level, shows that the Mn is in the divalent state. Further analysis of both the spectral shape and the branching ratio of this spectrum shows the crystal-field splitting of the d^0 ion to be between 1 and 1.5 eV. The ideal formula of saneroite, assuming pentavalent vanadium as confirmed in Fig. 1, indicates that both di- and trivalent Mn are required at a ratio of nine Mn^{2+} ions to one Mn^{3+} ion. While the spectrum of saneroite (BM 1984,868), in Fig. 2, initially appears to be very similar to that of schorlomite, the 'shoulder' on the high-energy side of the main peak, at ~641 eV, and the second peak at ~643 eV are both relatively more intense in the saneroite spectrum than in the schorlomite spectrum, revealing that a contribution is indeed required from Mn^{3+}.

Piemontite is a manganoan epidote in which it is generally thought that the Mn^{3+} replaces Al^{3+} or Fe^{3+} cations.

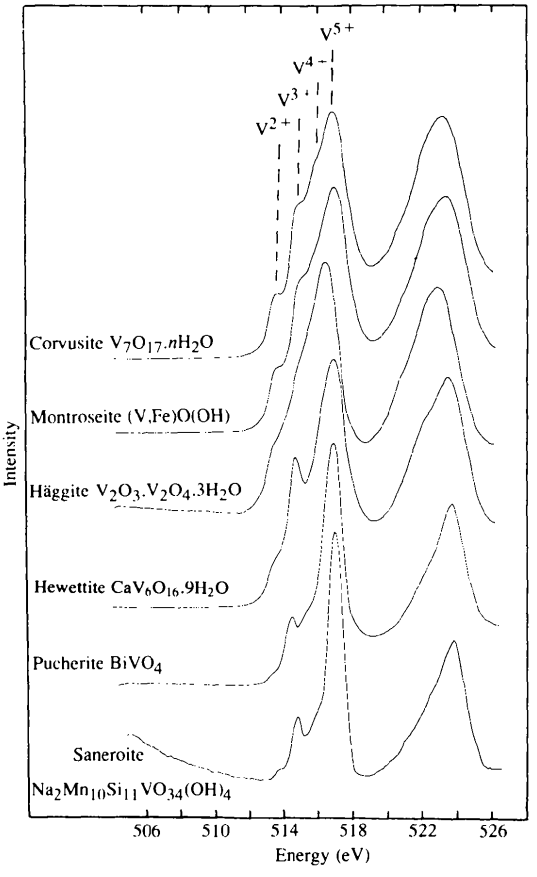

Figure 1
V 2p X-ray absorption spectra for a range of vanadium-bearing minerals. Relative energy positions of the L_3 absorption maxima for V^{2+}, V^{3+}, V^{4+} and V^{5+} are indicated (van der Laan & Kirkman, 1992). All specimens are from the collection of the Natural History Museum, UK, and are labelled as follows: corvusite (BM 1957,33), montroseite (BM 1956,200), häggite (BM 1963,663), hewettite (BM 1972,461), pucherite (BM 45983) and saneroite (BM 1984,868).

The spectrum of piemontite (BM 68608) in Fig. 2, however, clearly shows that a significant proportion of Mn^{2+} is also present. Although the Mn^{2+} may be present in the octahedral sites, Bonazzi, Garbarino & Menchetti (1992) have previously reported that Mn^{2+} may be involved in a substitution in which it replaces the Ca^{2+} on the *A*1 site. The spectra for gaudefroyite and hollandite show the expected oxidation states of Mn^{3+} with some Mn^{2+} in gaudefroyite and $Mn^{4+}$and Mn^{2+} in hollandite (BM 1909,182), although the proportion of divalent Mn is rather higher than expected in the spectrum of the hollandite sample.

While the oxidation states identified in this study can generally be explained by varying site occupancies or charge-balancing substitutions, the work of Cressey *et al.* (1993) revealed the presence of Mn^{4+}, an oxidation state not required by the supposed stoichiometry, in the minerals vredenbergite, $(Mn,Fe)_3O_4$ (BM 1951,23), and jacobsite, $MnFe_2O_4$ (BM 1966,302). This was found to be due to partial alteration of these phases to pyrolusite, MnO_2, on grain boundaries and surfaces, and also on fractures and cleavage planes of the crystals. This highlights another serious problem for the mineralogist in that the majority of valence probes in routine use are bulk techniques. The use of high spatial resolution techniques for chemical imaging are currently being developed. These either utilize focused photon beams or exploit the technique of photo-electron emission microscopy (*e.g.* Tonner, 1991; Mundschau, 1991; Drummand, 1992). Such techniques are beginning to enhance the potential of 2*p* X-ray absorption spectroscopy greatly, enabling the study of both zoned and partially altered crystals.

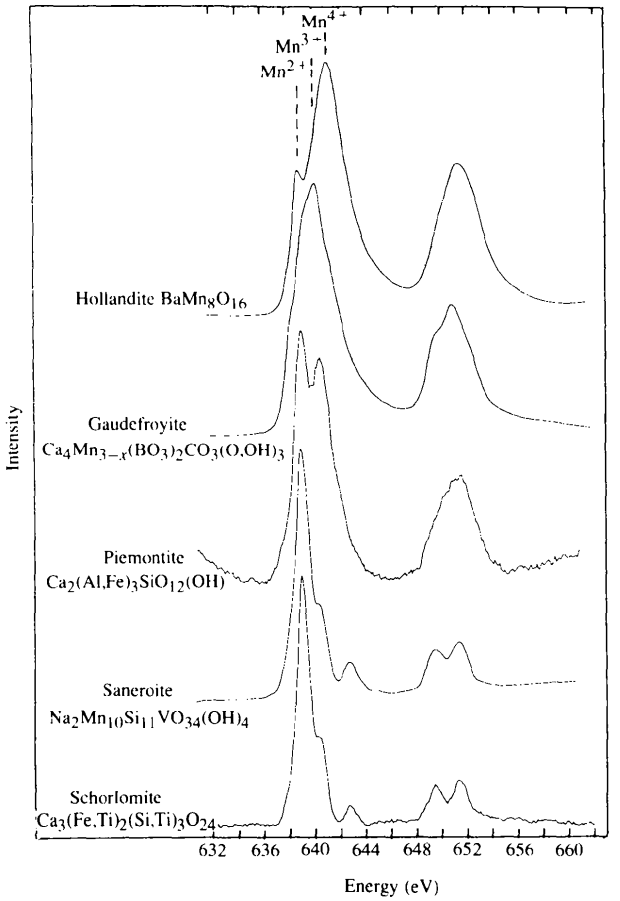

Figure 2
Mn 2*p* X-ray absorption spectra for a range of manganese-bearing minerals. Relative energy positions of the L_3 absorption maxima for Mn^{2+}, Mn^{3+} and Mn^{4+} are indicated (van der Laan & Kirkman, 1992). All specimens, except gaudefroyite, provided by L. A. J. Garvie, University of Glasgow, are from the collection of the Natural History Museum, UK, and are labelled as follows: hollandite (BM 1909,182), piemontite (BM 68608), saneroite (BM 1984,868) and schorlomite (BM 32025).

2.3. *Copper oxidation states*

In chemically complex sulfide minerals, transition metals enter a wide variety of site symmetries and possess a range of formal valency states which may vary with site occupancy and chemical substitutions. The situation is further complicated by prevalent defect states and the apparent stability of a wide range of non-stoichiometric compositions in several sulfide mineral types. Although copper with a formal valency of +1 and a ground state of $3d^{10}$ cannot give a 2*p* to 3*d* transition, hybridization to a $3d^9$ *s* state enables a low probability of 2*p* to 3*d* transitions to occur. van der Laan *et al.* (1992) showed, for a large range of monovalent Cu minerals, that the main L_3 peak occurs within the energy range 931.9–933.4 eV, whereas the L_3 peak for divalent Cu minerals occurs in the energy range 930.5–931.2 eV. Sarma *et al.* (1988) showed that the L_3 peak for trivalent copper, in the usual $2p^6\,3d^8$ ground state, occurs at about 941 eV. Thus, the energy positions of the absorption peaks in 2*p* spectra provide a means for the identification of Cu valence states in minerals.

3. Quantification of valence states

The correct identification of individual valence states of 3*d* transition metals within multivalent minerals is indeed important, however, the quantification of these valence ratios is of particular interest to mineralogists and geochemists. The understanding of disparate mineralogical phenomena such as thermodynamic properties, deprotonation and oxidation processes, and geothermometric and geobarometric considerations, all require a reliable knowledge of valence ratios. Such analyses of spectra from 2*p* XAS have been fully detailed by Cressey *et al.* (1993) and Schofield *et al.* (1994), and only a brief outline is given here. Convoluted profiles, representing the identified oxidation states, are simulated by summation of the calculated multiplet $L_{2,3}$ structures from van der Laan & Kirkman (1992) with appropriate site symmetries and crystal-field parameters. The remaining variables in this process are the valence ratio, line shape and width, and relative energy shift between the spectral components. The convoluted profiles are then compared with experimental spectra for the samples of interest.

3.1. $Ti^{3+}/\Sigma Ti$ ratio

The terrestrial mineral vuonnemite, whose ideal formula is $Na_5Ti^{3+}Nb_2(Si_2O_7)_2F_2O_2.2Na_3PO_4$, was believed to contain substantial Ti^{3+} by Ercit & Hawthorne (1994), based on long-range electroneutrality requirements and bond-valence calculations. The experimental and calculated Ti 2*p* XAS spectra of vuonnemite (BM1987,3) are shown in Fig. 3. The strong peaks at about 458, 460, 463.5 and 465.5 eV are all due to Ti^{4+}, while the features at about 459, 462 and 464.5 eV are due to Ti^{3+} (Schofield *et al.*, 1994). The $Ti^{3+}/\Sigma Ti$ ratio was estimated to be 0.63 (0.01) from the fit to the experimental profile intensity (*I*) using the following equation, appropriate for a single octahedral site for Ti:

$$I_{obs} = (10/9)[I_{Ti^{4+}O_h}(Ti^{4+}/\Sigma Ti)] + I_{Ti^{3+}O_h}[1 - (Ti^{4+}/\Sigma Ti)]$$

where the coefficient 10/9 is the ratio of *d* holes in the Ti^{4+} (d^0) and Ti^{3+} (d^1) configurations.

3.2. $Fe^{3+}/\Sigma Fe$ ratio

Cressey *et al.* (1993) demonstrated the sensitivity of this technique, and hence its applicability to trace elements, by identifying and subsequently quantifying the valence states of Fe in amethyst quartz, where the concentration of Fe is about 0.01%. Fig. 4 shows the experimental Fe $L_{2,3}$ spectrum for amethyst (BM 40868) from which it can clearly be seen that while both Fe^{2+} and Fe^{3+} are present, there is no evidence for Fe^{4+}, as proposed by many previous investigations. Using the equation

$$I_{obs} = (5/4)[I_{Fe^{3+}T_d}(Fe^{3+}/\Sigma Fe)] + I_{Fe^{2+}T_d}[1 - (Fe^{3+}/\Sigma Fe)]$$

in which *I* is the experimental profile intensity and the coefficient 5/4 represents the ratio of *d* holes and, appropriate for a single tetrahedral site, the $Fe^{3+}/\Sigma Fe$ ratio was found to be 0.32 (0.01). This was the first report identifying Fe^{2+} as the dominant Fe cation in amethyst; we have subsequently found that several different specimens of amethyst produce ratios close to 0.33, implying that some crystallographic control is operational in conjunction with crystal-chemical controls.

3.3. $Cu^{2+}/\Sigma Cu$ ratio

The quantification of the $Cu^{2+}/\Sigma Cu$ ratio is somewhat more complicated than for the other 3*d* transition metals. The integrated intensity for the absorption spectra for the other 3*d* transition-metal cations, as described by van der Laan & Kirkman (1992), is proportional to the number of 3*d* holes. While this is also true for Cu^{2+}, the 2*p* XAS spectra of Cu^{+} (nominally $3d^{10}$) results from hybridization with ligand orbitals and as a result cannot be directly compared in the same way as described above.

Pattrick *et al.* (1993) described and demonstrated a solution to this problem by comparing the integrated intensity of the divalent copper L_3 peak with a part of the monovalent copper spectrum in which the intensity is a measure of the delocalized *sd* density of states. Using a varied series of standard materials, and a range of mixtures of these standards, they obtained a transferable average intensity factor of 23 (Cu^{2+}/Cu^{+}) with a standard deviation of 5. Pattrick *et al.* (1993) then demonstrated the applicability

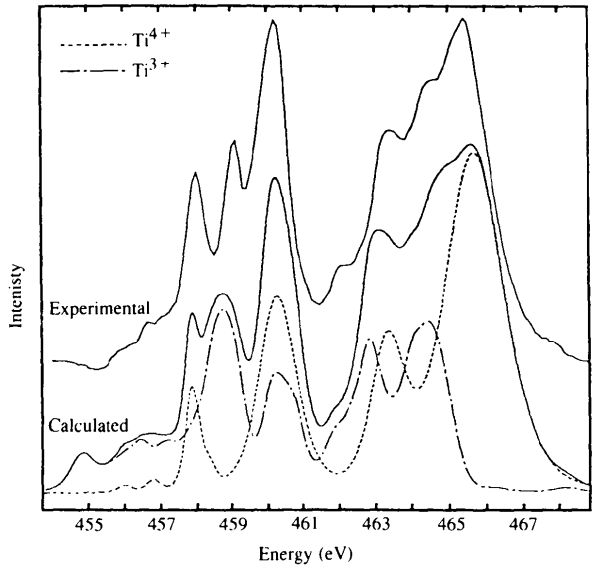

Figure 3
Experimental Ti 2*p* X-ray absorption spectrum of the mineral vuonnemite (BM 1987,3) (top) with the best-fit simulation assuming Ti^{4+} with $10Dq$ = 2.1 eV and Ti^{3+} with $10Dq$ = 2.0 eV, giving a $Ti^{3+}/\Sigma Ti$ ratio of 0.63 (after Schofield *et al.*, 1994).

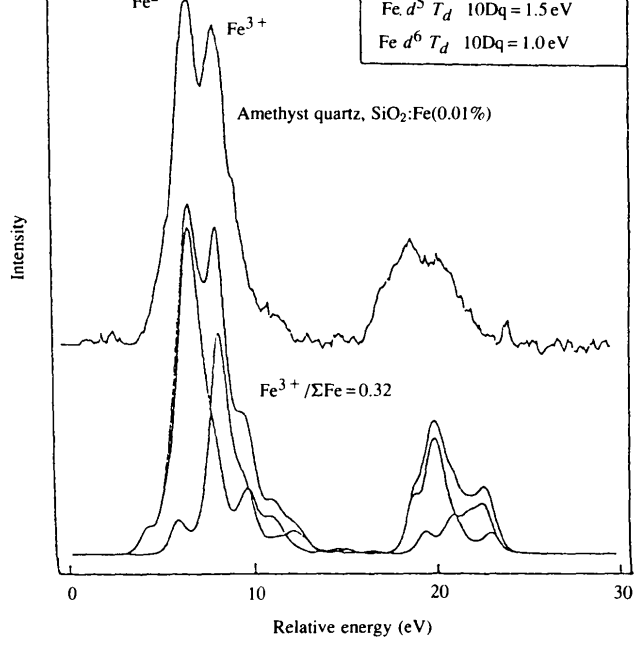

Figure 4
Experimental Fe 2*p* X-ray absorption spectrum of amethyst quartz (BM 40868) (top) with the best-fit simulation assuming Fe^{2+} with $10Dq$ = 1.0 eV and Fe^{3+} with $10Dq$ = 1.5 eV, giving an $Fe^{3+}/\Sigma Fe$ ratio of 0.32 (after Cressey *et al.*, 1993).

of this relationship by quantifying the Cu^{2+}/Cu^{+} ratios in a series of chemically complex natural and synthetic tetrahedrites.

4. Identification of different site symmetries

The site occupancies and symmetries of 3*d* transition-metal cations also play a significant role in determining mineral and melt properties. Many site occupancy models remain controversial principally due to the limited capabilities of established techniques. van der Laan & Kirkman (1992) showed that 2*p* XAS is also sensitive to site symmetries for the 3*d* transition-metal series and Schofield *et al.* (1993) were able to model the occupancies of two distinct Cu electronic sites across the $CuWO_4$–$ZnWO_4$ solid solution using Cu 2*p* XAS. We will further demonstrate the potential of $L_{2,3}$ XAS using the example of Ti^{4+}.

Ti^{4+} (d^0) is predominantly found to reside in octahedral coordination, but is also known to exist in 5-coordination, as in the mineral fresnoite, $Ba_2TiSi_2O_8$ (Moore & Louisnathan, 1969), and in tetrahedral coordination in Ba_2TiO_4 (Bland, 1961) and $CsAlTiO_4$ (Gatehouse, 1989). Fig. 5 shows the calculated spectrum for Ti^{4+} in T_d and O_h symmetry ($10Dq$ = 2.0 eV) along with the experimental spectrum of fresnoite ($Ba_2TiSi_2O_8$) and from this it can be seen that there are significant differences between the spectra allowing the identification of site symmetries even in multi-site scenarios. Simply by adopting the principles of the valence-ratio quantification method we are able to quantify the proportions of different coordinate sites identified in a given sample.

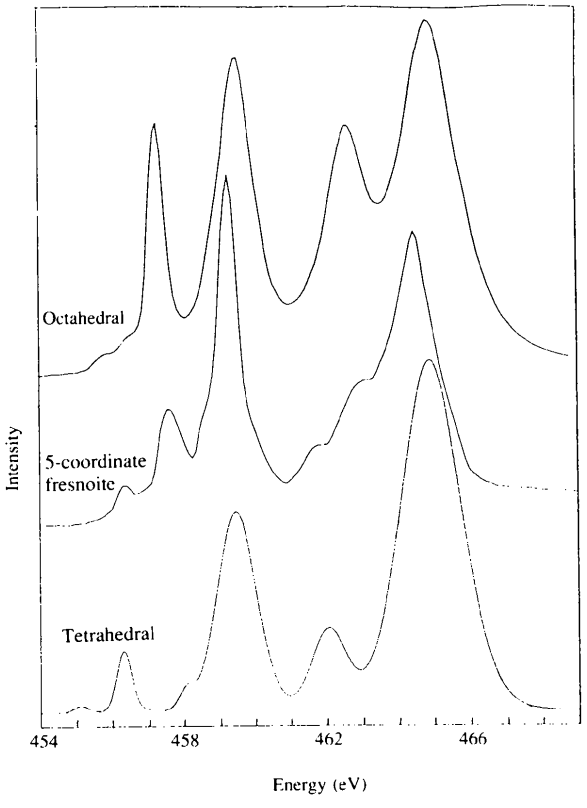

Figure 5
The calculated Ti 2*p* X-ray absorption spectra in octahedral symmetry (top) and tetrahedral symmetry (bottom) with the experimental spectrum of the mineral fresnoite in which the Ti^{4+} is 5-coordinate (centre).

5. Conclusions and future developments

We have demonstrated the potential of 2*p* XAS as a sensitive, element-specific site and valency probe for use with geological materials. By monitoring the electronic structure of the 3*d* transition metals present in both minerals and glasses, we are able to quantify the valence and site ratios, a result which cannot be reliably obtained from *K*-edge EXAFS of these elements. The element specificity of X-ray absorption spectroscopy should enable reliable information to be directly gleaned from natural material without the need to depend on synthetic and analogue samples which might be required by other techniques. Although we have concentrated on geological specimens, this technique has the potential to be a powerful probe of valency and site occupancy for all solid-state and materials scientists studying the 3*d* transition metals.

The modelling of spectra is still in its early stages of development. In the future we will be able to improve on the currently available methods by taking into account effects such as non-cubic crystal fields, temperature, hybridization and solid-state effects. While the inclusion of such effects will undoubtedly produce better theoretical fits with the experimental spectra, it is unlikely that the quantified ratios we are already able to determine will be altered significantly. Electron yield detection, currently used in these studies, probes depths of between 50 and 100 Å, giving surface sensitivity which may prove both advantageous or disadvantageous depending on the nature of the information sought. The development of fluorescence and energy-dispersive detectors will improve both the probing depth and the ability to remove spectral components resulting from intergrowths of secondary phases, while microbeam methods will allow the analysis of zoned single crystals and grain boundaries.

References

Bland, J. A. (1961). *Acta Cryst.* **14**, 875–881.
Bonazzi, P., Garbarino, C. & Menchetti, S. (1992). *Eur. J. Miner.* **4**, 23–33.
Chen, C. T. & Sette, F. (1989). *Rev. Sci. Instrum.* **60**, 1616–1621.
Cressey, G., Henderson, C. M. B. & van der Laan, G. (1993). *Phys. Chem. Miner.* **20**, 111–119.
Drummand, I. W. (1992). *Microsc. Anal.* (March), 29–32.
Ercit, T. S. & Hawthorne, F. C. (1994). *Can Miner.* Submitted.
Evans, H. T. (1989). *Can. Miner.* **27**, 181–188.
Evans, H. T. Jr & Mrose, M. E. (1960). *Am. Miner.* **45**, 1144–1166.
Forbes, P. & Dubessy, J. (1988). *Phys. Chem. Miner.* **15**, 438–445.

Gatehouse, B. M. (1989). *Acta Cryst.* C**45**, 1674–1677.
Groot, F. M. F. de, Figueirdo, M. O., Basto, M. J., Abbate, M., Petersen, H. & Fuggle, J. C. (1992). *Phys. Chem. Miner.* **19**, 140–147.
Henderson, E. P. & Hess, F. L. (1933). *Am. Miner.* **18**, 195–205.
Laan, G. van der (1990). *Phys. Rev. B*, **41**, 12366–12368.
Laan, G. van der & Kirkman, I. W. (1992). *J. Phys. Condens. Matter*, **4**, 4189–4204.
Laan, G. van der, Pattrick, R. A. D., Henderson, C. M. B. & Vaughan, D. J. (1992). *J. Phys. Chem. Solids*, **53**, 1185–1190.
Moore, P. B. & Louisnathan, S. J. (1969). *Z. Kristallogr.* **130**, 438–448.
Mundschau, M. (1991). *Synchrotron Rad. News*, **4**(4), 29–34.
Padmore, H. A. & Warwick, T. (1994). *J. Synchrotron Rad.* **1**, 27–36.
Pattrick, R. A. D., van der Laan, G., Vaughan, D. J. & Henderson, C. M. B. (1993). *Phys. Chem. Miner.* **20**, 395–401.
Sarma, D. D., Strebel, O., Simmons, C. T., Neukirch, U., Kaindl, G., Hoppe, R. & Muller, H. P. (1988). *Phys. Rev. B*, **37**, 9784–9787.
Schofield, P. F., Henderson, C. M. B., Redfern, S. A. T. & van der Laan, G. (1993). *Phys. Chem. Miner.* **20**, 375–381.
Schofield, P. F., Henderson, C. M. B., Searle, B. G., Cressey G., van der Laan, G. & Hawthorne, F. C. (1994). *Eur. J. Miner.* Submitted.
Tonner, B. P. (1991). *Synchrotron Rad. News*, **4**(2), 27–32.